Eur. Phys. J. B **3**, 485–496 (1998)

THE EUROPEAN PHYSICAL JOURNAL B

Depinning of a domain wall in the 2d random-field Ising model*

B. Drossel[1,a] and K. Dahmen[2,b]

[1] Department of Theoretical Physics, University of Manchester, Manchester M13 9PL, England
[2] Lyman Laboratory of Physics, Harvard University, Cambridge, MA02138, USA

Received: 13 February 1998 / Accepted: 30 March 1998

Abstract. We report studies of the behaviour of a single driven domain wall in the 2-dimensional non-equilibrium zero temperature random-field Ising model, closely above the depinning threshold. It is found that even for very weak disorder, the domain wall moves through the system in percolative fashion. At depinning, the fraction of spins that are flipped by the proceeding avalanche vanishes with the same exponent $\beta = 5/36$ as the infinite percolation cluster in percolation theory. With decreasing disorder strength, however, the size of the critical region decreases. Our numerical simulation data appear to reflect a crossover behaviour to an exponent $\beta' = 0$ at zero disorder strength. The conclusions of this paper strongly rely on analytical arguments. A scaling theory in terms of the disorder strength and the magnetic field is presented that gives the values of all critical exponent except for one, the value of which is estimated from scaling arguments.

PACS. 75.60.Ch Domain walls and domain structure – 05.70.Ln Nonequilibrium thermodynamics, irreversible processes – 47.55.Lh Flows through porous media

1 Introduction

The random-field Lenz-Ising model is one of the simplest examples of random media, with applications far beyond magnetic systems (for a recent review, see [1]). Recently interesting nonequilibrium aspects have been studied, such as the field driven motion of a single domain wall [2–9], domain coarsening in rapidly cooled magnetic systems, where the domain wall motion is curvature driven [10], and hysteresis, with many interacting driven domain walls [11]. Studies of a single driven domain wall were found to describe fluid invasion in porous media [2]. These studies fall into the large class of interface depinning problems, which also include charge density wave depinning, contact line depinning, earthquakes, and domain wall depinning in magnets [12,13]. In these systems, second order dynamical phase transitions were found as the driving force F surpasses some critical threshold value F_c, at which the interface becomes depinned, and starts to propagate through the system at a velocity $v \sim (F - F_c)^{\phi}$ with a critical exponent ϕ.

In previous work on a single field driven domain wall in the random field Ising model in three dimensions, three different modes of interface propagation close to the depinning threshold were identified [7]: For weak, bounded disorder, the marginally stable interface at F_c is facetted, for intermediate disorder it is self-affine, and for large disorder it is self-similar. In the "faceted growth" [2,3,7,9] the interface propagates just as in the absence of disorder, penetrating the medium completely, with a roughness exponent $\zeta = 0$ at the depinning threshold. This type of interface motion can occur in any dimension, but only for a narrow, bounded distribution of random fields, not for unbounded (Gaussian) distributions of random fields. The existence of this phase is lattice dependent [8].

In the self-affine regime, which was seen in 3-dimensional simulations with bounded and Gaussian distribution of random fields [7,14], neighbouring interface segments proceed coherently, and the interface has a roughness exponent smaller than one. Overhangs and "bubbles" (*i.e.*, uninvaded domains left behind by the advancing interface) occur only below a certain length scale and can therefore be neglected on long length scales, where the interface can be described by a single-valued function. The critical properties of the interface near the depinning threshold were derived analytically starting from a continuum model with a single-valued function for the interface, and performing a renormalization group calculation, and ϵ expansion around the upper critical dimension which is 5 [4,5]. This ϵ expansion yields the roughness exponent $\zeta = (5 - d)/3$ for a $d - 1$-dimensional domain wall in a in a d-dimensional system, which is argued to be exact to all orders in perturbation theory [5], however, numerical simulations show deviations from this prediction [6]. If the renormalization group result $\zeta = (5-d)/3$ is indeed exact, it implies that $d = 2$ is the lower critical dimension, where

* Dedicated to F. Schwabl on the occasion of his 60th birthday.

[a] e-mail: drossel@a13.ph.man.ac.uk
[b] e-mail: dahmen@cmt.harvard.edu

the ansatz of an interface without overhangs at large scales breaks down and conventional correlated depinning does not occur any more. Anisotropies in the medium may give rise to further depinning universality classes [15].

For strong disorder, the invading phase advances in a percolation-like manner, following routes of particularly high random field values. When the driving force is at the depinning threshold, the invading phase penetrates only a vanishing volume fraction of the invaded medium, just as a spanning cluster in percolation theory [2,7]. Numerical results for the fractal dimension of the invaded volume and the external hull of the interface suggest that this system is in the same universality class as uncorrelated site percolation [2,7]. When the disorder strength is decreased, the percolation pattern coarsens, and the thickness of the percolation fingers increases and diverges at the critical disorder R_c which marks a transition to conventional (coherent, self-affine) depinning [2,7,8]. While in three dimensions $R_c > 0$, in 2 dimensions simulation results seem to indicate that this divergence of the finger width occurs only in the limit of zero disorder ($R_c = 0$) [2,8], suggesting again that $d = 2$ plays the role of a lower critical dimension.

This result however so far is only an indication. Within the numerical accuracy of the 2-dimensional simulations a nonzero R_c could not definitely be ruled out, and the issue is still controversial. While 2 is the lower critical dimension for the equilibrium random-field Ising model, there is no obvious reason that this result should be transferable to a nonequilibrium situation [16]. There are other nonequilibrium problems with similar hurdles to establishing the lower critical dimension. An example are hysteresis loops in the 2-dimensional random-field Ising model with many interacting interfaces. Numerical simulations, even of rather large systems (up to $30\,000^2$), seem to converge towards zero critical disorder, but so far do not definitely rule out the possibility of a phase transition at nonvanishing disorder value either [11].

Another open question is whether the type of correlated percolation found for domain-wall motion in the random-field Ising model does indeed belong to the same universality class as conventional uncorrelated site percolation. In fact, while the fractal dimension of the external perimeter of a site percolation cluster is 4/3 [17], in agreement with the dimension found for the magnetic interface [2], the fractal dimension of the hull (which is the perimeter that one measures stepping along occupied sites) of a percolation cluster is 7/4 [17], which is different from the value 4/3 for the RFIM interface (see below).

The main purpose of this paper is to present new support for the conclusion that 2 is indeed the lower critical dimension for the transition described above, with $R_c = 0$, and to give analytical and numerical arguments that in 2 dimensions on sufficiently long length scales (even for very narrow Gaussian distribution of random fields) the interface propagates in the self-similar mode, characterized by site percolation critical exponents. In contrast to previous simulations of the pinned interface where the depinning point is approached from below, here it is approached from *above* with focus on the volume fraction m filled by the invading phase as a function of the strength of the driving force (*i.e.*, the magnetic field). Since m vanishes at percolation-like depinning, but is nonzero at correlated depinning, it can be used as an "order parameter" for the phase transition between the two behaviours. Scaling forms for m, and the width and length and fractal dimension of the interface, and other quantities, are conjectured and tested numerically, and ultimately justified by a scaling theory. Analytical arguments based on the properties of the domains of unflipped spins left untouched by the proceeding interface give strong support for a phase transition at zero disorder. They also show that the width of the critical region decreases towards zero as the strength of the disorder vanishes. Mappings of the model for several values of the parameters onto other percolation models with (supposedly) known values for the critical exponents confirm that the growth of m above depinning is characterized by the conventional percolation exponent $\beta = 5/36$. The numerical data are compatible with a critical point at zero random field, and reflect a crossover from the percolation critical exponent $\beta = 5/36$ very close to depinning to $\beta' = 0$ further away. The roughness exponent characterizing the interface and the fractal dimension of the interface are $\zeta = 1$ and $d_f = 4/3$. Building on these results, we conjecture a scaling theory for the critical behaviour in $d = 2$ dimensions in the limit of small disorder. Except for one exponent, the exact values of all other exponents can be postulated, and for the remaining exponent, an approximate result is obtained from scaling arguments.

The outline of the remainder of the paper is as follows: in Section 2, the model is introduced. In Sections 3 and 4, the numerical and analytical results are given. The final section contains a discussion of the results and ideas for further work.

2 The model

The random-field Ising model is defined by the following Hamiltonian

$$\mathcal{H} = -J \sum_{\langle i,j \rangle} S_i S_j - \sum_i (h_i + H) S_i \,. \tag{1}$$

The field H is the external field, $\langle i, j \rangle$ denotes nearest-neighbour pairs, and the spin variable S_i assumes the values ± 1. In most discussions of the model, the probability distribution of the random fields $\{h_i\}$ is a Gaussian

$$p(h_i) = \frac{\exp\left[-h_i^2/2R^2\right]}{\sqrt{2\pi}R} \tag{2}$$

of width R. Random fields at different sites are taken to be uncorrelated.

The subsequent discussion is limited to a 2-dimensional system on a square lattice at zero temperature. Initially all spins are taken to be pointing down ($S_i = -1$), except for one column of up-spins at the

left boundary of the system, which, for convenience are given an infinitely positive random field h_i. The upper and lower sides of the system are connected by periodic boundary conditions. For a given value H of the external magnetic field, successively all those spins are flipped up that have a positive local field $J\sum_j S_j + H + h_i$ and at least one flipped "up" neighbour (*i.e.* those spins immediately neighbouring the successively propagating interface of the growing cluster of up spins). For negative or small positive values of the external field H, the interface of up spins cannot proceed far and stops after a small number of steps. For large positive H, on the other hand, the propagating interfaces runs from left to right through the entire system, leaving behind only small domains of unflipped spins. For values H below some critical value $H_c(R)$, the order parameter m vanishes, *i.e.*, $m = 0$, while it becomes finite for $H > H_c(R)$. If at $R > 0$ the spin-flip avalanche proceeds percolation-like, the transition from $m = 0$ to $m > 0$ is continuous with

$$m \simeq A(R)(H - H_c(R))^{\beta}\,, \tag{3}$$

with some prefactor A that depends on the width of the random field distribution. If the invaded area has the same critical properties as a spanning cluster in uncorrelated site percolation (in 2-dimensions), as suggested in [2,8], then $\beta = \beta_{perc} = 5/36 \simeq 0.139$. If 2 is the lower critical dimension for the transition from percolation-like to correlated depinning, we expect that this percolation-like behaviour persists even for arbitrarily small randomness R on sufficiently long length scales and at sufficiently small magnetic fields. On the other hand, if there is a phase transition to correlated depinning for some finite random field strength R_c, then the magnetization is expected to display a jump from 0 to some finite value m at at $H = H_c(R)$ for $R < R_c$. In this paper, we will argue for $R_c = 0$ and the scenario of equation (3) for $R > 0$ and H sufficiently close to depinning $H_c(R)$ on sufficiently long length scales. If

$$H + h_i + (2n-4)J > 0 > H + h_i + (2(n-1)-4)J\,,$$

the local field at site i becomes positive (causing S_i to flip up) when the nth nearest neighbour flips up. It is useful to define the probabilities

$$\rho_n = \int_{(4-2n)J-H}^{(6-2n)J-H} p(h_i)dh_i \tag{4}$$

that a spin flips as soon as n of its nearest neighbours are flipped. Since we only allow spins connected to the advancing interface to flip, (*i.e.* isolated spins remain unflipped), we absorb ρ_0 into ρ_1. For the advancement of the avalanche, there is no difference between a site that flips only when all four neighbours are flipped, and a site that does not flip even with four flipped neighbours, so we include in ρ_4 all sites with $h_i < -H - 2J$. Subsequently, for convenience, we describe the system in terms of these four probabilities instead of H/J and R/J, as done also by other authors [18]. They span a three dimensional parameter space, since $\rho_1 + \rho_2 + \rho_3 + \rho_4 = 1$. The plane

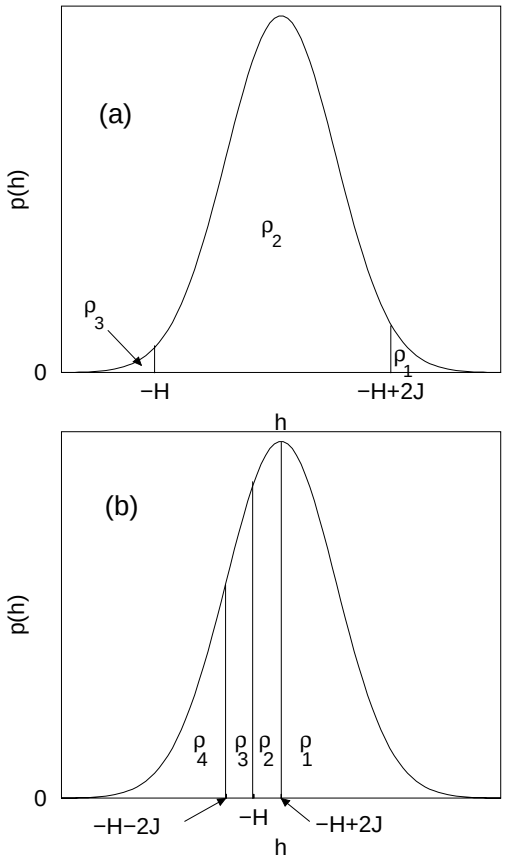

Fig. 1. The densities ρ_n for (a) small R/J and (b) large R/J, represented as areas under the Gauss-distribution for the random field. In (a), the density ρ_4 is so small, and its area is so far to the left, that it is not shown in the figure.

spanned by H/J and R/J represents a cut through this space. Changing the external field H for a given distribution of random fields corresponds to moving along a line given implicitely by equation (4). There exists a critical surface in the parameter space that separates the region with $m = 0$ from the region with $m > 0$, which contains the line $H_c(R)$.

We begin by presenting some fundamental properties of the two limiting cases of weak and strong disorder. Figure 1 illustrates the relation between the model parameters and the densities ρ_n. For small R/J (weak disorder), regions of a given n are wide compared to R/J, and one or two neighbouring values of n dominate the system, while for large R/J (strong disorder), the regions of given n are narrow, and the two boundary regions for $n = 1$ and $n = 4$ dominate. Obviously, in the limit $R/J \to \infty$, the model corresponds to a site percolation system, where $\rho_4 = 1 - \rho_1$. Knowing the value of the site percolation threshold, $\rho_1^c \simeq 0.59$, we can immediately give an implicit expression for the critical magnetic field H_c,

$$\rho_1^c = \int_{2J-H_c}^{\infty} p(h_i)dh_i, \qquad R/J \to \infty.$$

In the limit of small R/J, depinning occurs when H is

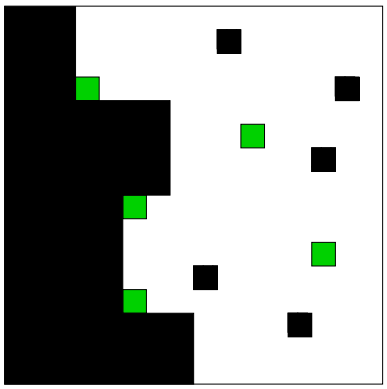

Fig. 2. The phase boundary between up spins (large black area) and down spins (remaining area). The down spins ar colour coded depending on whether they flip as soon as one (black), two (white), or three neighbours (grey) are flipped.

such that ρ_2 is close to one, and $\rho_1 \simeq \sqrt{\rho_3}$. To understand this, consider a stable phase boundary between the spin up and spin down regions, as drawn in Figure 2. The invaded area (spin up) is indicated in black, as well as those spins that will flip as soon as one of their neighbours is flipped. The grey sites will only flip when three neighbours are flipped and sit therefore in the corners of the boundary. White sites will flip when two neighbours are flipped. The depinning transition occurs when there exists no stable boundary that spans the system. Let us call a possible boundary "pinning path". The following construction of a pinning path gives a good estimate for the relation between ρ_1 and ρ_3 at the depinning threshold: consider a system with all spins down. Now start at the bottom of the system at a bond that has no black right-hand neighbour and make a step upward. The path can proceed in the same direction as long as there are no black right-hand neighbours. It can turn left anywhere (if this does not lead to a black right-hand neighbour), but can turn right only at grey sites. Since the path is not allowed to intersect itself, and since it must ultimately arrive at the top end of the system, the mean number of right turns must equal the mean number of left turns. Thus, for each black site that is avoided by a left turn, there must be a grey site, where a right turn can be made. Since the density of black sites is ρ_1, the path has on an average $1/\rho_1$ opportunities to turn left before encountering the next black site. After the left turn, the probability of encountering a grey site before encountering a black site, is

$$p_{surv} = \rho_3/(\rho_3 + \rho_1)\,. \tag{5}$$

The path can survive when this probability, multiplied by the number of turning opportunities, is not smaller than 1, *i.e.*, $\rho_3/\rho_1(\rho_3 + \rho_1) \geq 1$, leading to

$$\rho_3 = \rho_1^2/(1 - \rho_1)$$

at the depinning threshold. For small values of R (weak random fields), ρ_3 and ρ_1 are also small, and $\rho_3 \simeq \rho_1^2$ at the depinning threshold. In [8], the relation $\rho_3 \propto \rho_1^{1.75\pm0.05}$ was obtained numerically (for a rectangular distribution of random fields), however, an exponent 2 can also be reconciled with their Figure 4, when the smaller slope in the lower part of the plot is ascribed to finite-size effects. In [19], the relation $\rho_3 \simeq (2/3)\rho_1^2$ was derived, which agrees with the one given here apart from the prefactor. The authors of [19] obtained their relation from the condition that an initially straight interface along the first column of sites can invade the same number of sites in the second column of a 2-column system as in the third column of a three-column system. The prefactor should therefore change when more columns are taken into account. The argument presented in this paper does not consider the possibility of having two right (or left) turns in sequence, which, however, occurs by a factor $\rho_3/(\rho_1 + \rho_3)$ less often than alternating turns and makes therefore a negligible contribution to the above calculation in the limit $\rho_1 \to 0$. The argument also neglects possible correlations between different pinning paths starting at the same initial point. Taking these into account will probably change the prefactor. Irrespective of the prefactor, however, we can easily see that the density ρ_4 is negligible in the limit of small disorder: a short calculation gives the approximate result $\lim_{R\to 0} H_c(R) \simeq 2(2 - \sqrt{2})J \simeq 1.172J$ (also derived in [19]), leading to

$$\rho_3 \simeq (R/2.94J)\exp[-1.373J^2/2R^2]$$

and

$$\rho_4 \simeq (R/7.95J)\exp[-10.06J^2/2R^2]$$

at depinning threshold. Thus, the ratio ρ_4/ρ_3^4 becomes arbitrarily small for small disorder, which means that clusters of four grey sites forming a 2×2-square occur far more often than isolated sites that do not flip with three flipped neighbours. Since both play the same role in the system by blocking an avalanche even when surrounded by it on three sides, and since their size difference is irrelevant on long length scales, the neglection of ρ_4 does not change any properties of the system in the limit of small disorder.

To conclude this section, let us note that in addition to pinning paths that span the system and separate the invaded from the non invaded area, there exist pinning paths that are closed loops, delimiting unflipped domains within the invaded region.

3 Numerical results

Earlier numerical studies [2,8] used a quadratic system of L^2 sites in which the magnetic field H was increased incrementally, allowing the system to relax after each (adiabatic) increase. The system size dependent critical field $H_c(R, L)$ at which the invading spin-up phase first reached the right boundary of the system, was seen to converge towards a constant value $H_c(R)$ as L was increased. Information about the critical field, the fractal dimension of the invading cluster, and its perimeter were obtained upon approaching the depinning threshold from below.

The present work, in contrast, is mainly concerned with the behaviour of the fraction m of flipped spins *above*

Fig. 3. The invaded area (black) for $L = 400$ in the low disorder regime ($\rho_4 = 0$), slightly below depinning, with (a) $\rho_3 = 0.2$ and $\rho_1 = 0.43 < \rho_1^c(0.2) \simeq 0.4345$ and (b) $\rho_3 = 0.05$ and $\rho_1 = 0.2236 < \rho_1^c(0.05) \simeq 0.226$. L is the linear system size in the vertical direction. Roughly speaking, in the low disorder regime, smaller ρ_3 corresponds to smaller disorder, and $(\rho_1 - \rho_1^c)$ corresponds to $(H - H_c(R))$.

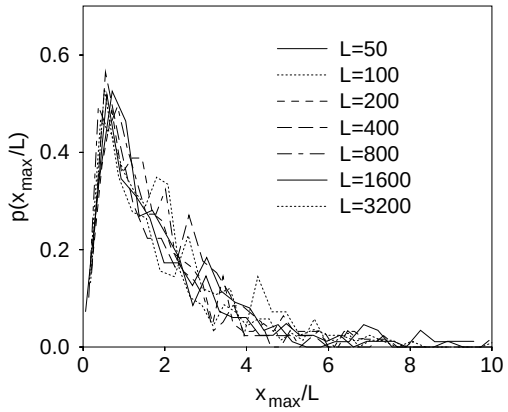

Fig. 4. Probability density for the position of the most advanced site of the pinned interface, for $\rho_3 = 0.05$ and $\rho_1 = 0.226 \simeq \rho_1^c(0.05)$. The collapse of the curves indicates that $\zeta = 1$.

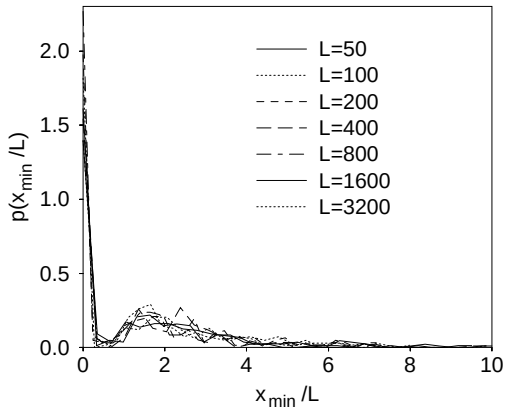

Fig. 5. Probability density for the position of the most retarded site of the pinned interface, for $\rho_3 = 0.05$ and $\rho_1 = 0.226 \simeq \rho_1^c(0.05)$. The collapse indicates that $\zeta = 1$.

the depinning threshold $H > H_c(R)$, focusing on the question whether m goes to zero continuously or discontinuously at depinning, and on the value of the critical exponent β. For this purpose, the external magnetic field (or, equivalently, the densities ρ_n) was set to a fixed value throughout a simulation run, and the interface was allowed to advance in a system of height L until it either came to a halt, or until it reached a cutoff distance which we chose to be *ca.* 10.5 L. Memory was allocated dynamically, and the system was updated by flipping all spins with positive local field along the interface. The following quantities were measured for various values of the system height L, and averaged over up to 250 realizations of the disorder: (i) the position of the most advanced and most retarded site, and the mean position of the interface, as well as the interface length at the moment where it came to a stop (if it did so before running over the maximum allowed distance). (ii) The fraction of spins flipped by the avalanche (disregarding the first $L/2$ columns, where the interface had not yet reached its stationary behaviour, and the last columns that were only partially invaded by the interface). (iii) The size distribution of the patches of unflipped spins left behind by the advancing interface. Before evaluation, these patches were allowed to relax, which is realistic for a magnetic system, but not for fluid invasion in a porous medium, where trapped regions cannot shrink. To study the low disorder regime, in our simulations we set ρ_4 to zero and ρ_3 to some small fixed value $\rho_3 = 0.2, 0.1$, or 0.05. ρ_1 was chosen close to the depinning threshold $\rho_1^c(\rho_3)$. The snapshots in Figure 3 show two pinned invasion patterns for two different values of the disorder (ρ_3), at ρ_1 slightly below the respective depinning threshold $\rho_1^c(\rho_3)$.

Two characteristic trends can be discerned for decreasing ρ_3 (*i.e.* decreasing random field strength R): the length of straight front segments increases, and the number of unflipped domains in the invaded area decreases. The first feature was explained in the previous, and the second feature will be explained in the following section. First, however, let us give more details of the simulation results.

3.1 Properties of the interface ($\zeta = 1$ and $d_f = 4/3$), and determination of the critical value $\rho_1^c(\rho_3)$ in the low disorder regime

Figures 4 and 5 show the probability density $p(x_{max}, L)$ for the position x_{max} and x_{min} of the most advanced and most retarded site of the interface for $\rho_3 = 0.05$ and

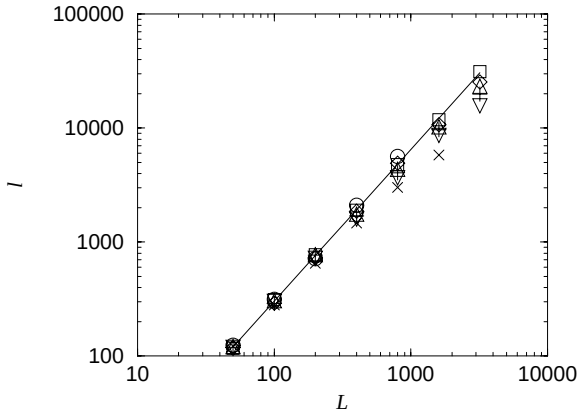

Fig. 6. The length of the interface l as function of L, for $\rho_3 = 0.1$ and ρ_1 =0.315 (circle), 0.317 (square), 0.318 (diamond), 0.319 (triangle up), 0.32 (plus), 0.322 (triangle down), and 0.325 ($\times$). The straight line is a power law fit to the $\rho_1 = 0.317 \simeq \rho_1^c(0.1)$ data, with an exponent 1.332.

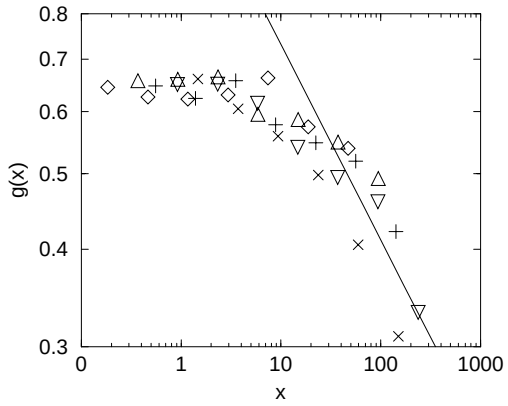

Fig. 7. The scaling function $g(x)$ for the interface length. The symbols are the same as in the previous figure. The straight line is a power law with exponent $-1/4$.

$\rho_1 = 0.226 \simeq \rho_1^c(0.05)$, scaled by the system height L. At depinning one expects the scaling behaviour $p(x_{max}, L) \sim f_1(x_{max}/L^\zeta)$ with a universal roughness exponent ζ and a universal scaling function f_1. Analogously, $p(x_{min}, L) \sim f_2(x_{min}/L^\zeta)$ with a universal scaling function f_2. The curves for different values of L collapse nicely, indicating that the system is indeed at the depinning threshold, *i.e.*, $\rho_1 = \rho_1^c(\rho_3)$, and $\zeta = 1$.

For larger values of ρ_1, (*i.e.* $H > H_c(R)$) the peak of the curves moves to the right with increasing L, and a nonvanishing fraction of all interfaces do not get stuck before reaching the cutoff distance $10.5L$ (especially for large values of L), since the system is above the depinning threshold. For smaller values of ρ_1, *i.e.* below the depinning threshold, the percentage of interfaces that remain attached to the first column increases with increasing L. Other values of ρ_3 give similar results. At depinning, one expects the mean thickness of the interface, defined as the number of columns spanned by the interface after it got stuck, to also scale as L^ζ. For the parameter values of Figures 5 and 4 this was verified with $\zeta = 1$. Once the interface has reached this mean asymptotic thickness of the order L, it becomes pinned with equal probability at any moment. This is reflected by the exponential tails of the scaling functions in Figures 4 and 5.

Figure 6 shows the mean length l of the pinned interface as function of L for different values of ρ_1, at fixed $\rho_3 = 0.1$. This length is the number of flipped spins that constitute the nearest-neighbour connected interface, *i.e.* the number of sites of the pinning path described in Section 2. Only interfaces with $x_{min} > L/2$ and $x_{max} < 10.5L$ were considered. The expected scaling form is $l \sim L^{d_f} g((\rho_1 - \rho_1^c(\rho_3))L^{1/\nu})$ with universal scaling function g, correlation length exponent ν, and fractal dimension d_f. At the critical threshold $\rho_1 \simeq 0.317 \simeq \rho_1^c(0.1)$ the points do indeed follow a power law. For nearby values of ρ_1, the critical behaviour is only visible for $L < \xi$ where $\xi \sim ((\rho_1 - \rho_1^c(\rho_3))/\rho_1)^{-\nu}$ is the correlation length. For larger L it crosses over to a different behaviour (linear in L in the case of $\rho_1 > \rho_1^c$). The straight line in the figure is a power-law fit to the critical data set, with exponent $d_f = 1.332 \pm 0.007$. Simulations for other values of ρ_3 give the same exponent $d_f = 1/\nu = 4/3$. For a percolation cluster, the exponent d_f is 7/4 [17]. The exponent 4/3 is retrieved, however, for a percolation cluster hull, when one allows steps to the next-nearest neighbours as well, thereby bridging the most narrow throats [17]. Since in our model sites with more flipped neighbours are more likely to flip also, narrow throats will be bridged with a certain probability, thus producing the exponent 4/3. The same exponent $d_f = 4/3$ characterizes also the fractal dimension of a self-avoiding random walk. This analogy becomes apparent in the limit of weak randomness (small ρ_3), where interfaces can be constructed by finding pinning paths that connect "grey" sites, as discussed in section 2 above. On sufficiently large scales, such paths are essentially self-avoiding random walks.

Figure 7 shows the collapsed data of Figure 6. On the horizontal axis, the scaling variable $x \equiv (\rho_1 - \rho_1^c(\rho_3))L^{4/3}$ is plotted, and on the vertical axis $l/L^{4/3}$, which is expected to be identical to the scaling function $g(x)$ defined above. One can see that the scaling function is constant for small x, and decays with $x^{-1/4}$ for large x. This decay corresponds to a linear dependence of l on L. The data points to the largest value of ρ_1 are already outside the scaling regime. The scattering of the other points is due to not too good statistics.

3.2 The exponent β

Figure 8 shows the order parameter m as function of $(\rho_1 - \rho_1^c(\rho_3))/\rho_1$ for $\rho_3 = 0.2$, 0.1, and 0.05. Only those data points are shown that are not affected by finite-size effects. (When finite-size effects are present, the fraction of flipped spins decreases with increasing system size. The reason is that only the area behind the interface was evaluated (not taking into account the first $L/2$ columns), which cannot contain unflipped regions larger than L and has therefore less unflipped spins for smaller system size.) With the maximum system height $L = 3200$ used in the

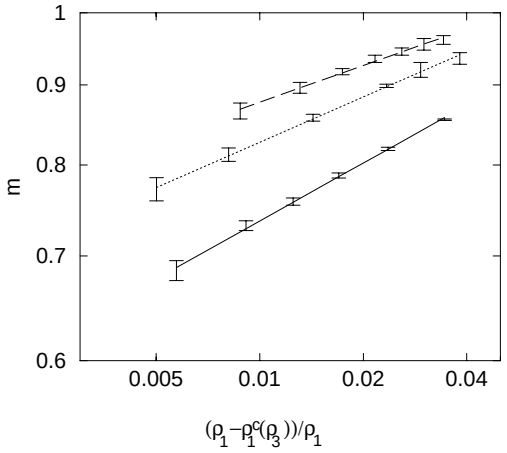

Fig. 8. The fraction of spins flipped by the avalanche as function of the distance from the critical density $\rho_1^c(\rho_3)$, for $\rho_3 = 0.2$ (solid), 0.1 (dotted), and 0.05 (dashed) for a system height up to $L = 3200$. The measured data points sit in the center of the error bars, and the error bars have a length of two times the standard deviation. The lines are a power-law fits to the data, with the exponents $\beta = 0.124$, 0.096, and 0.076. (Note that for percolation $\beta_{perc} = 0.139$.)

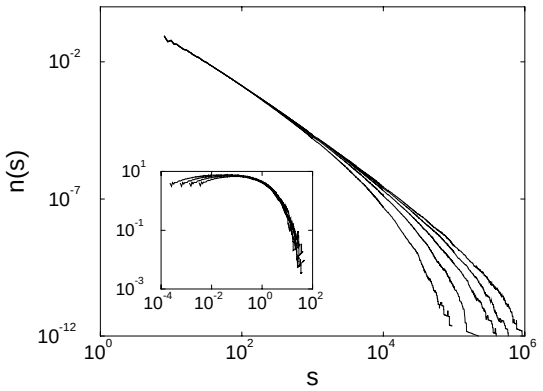

Fig. 9. Size distribution of unflipped regions for $\rho_3 = 0.2$ and $\rho_1 = 0.4385$, 0.44, 0.442, 0.445, and 0.45 (from right to left). $\rho_1^c(\rho_3 = 0.2) = 0.4345 \pm 0.005$. The inset shows a collapse of these data, plotting $s^\tau n(s)$ versus $((\rho_1 - \rho_1^c)/\rho_1)^{\sigma_n} s$ with $\tau = 1.85$, $\sigma_n = 1.8$, and $\rho_1^c = 0.437$.

simulations, the depinning threshold could not be approached closer than shown in Figure 8. As the log-log plot shows, the data points can be fitted within the error bars by a power law

$$m \propto ((\rho_1 - \rho_1^c(\rho_3))/\rho_1)^\beta \tag{6}$$

with an exponent $0.076 \leq \beta \leq 0.124$ that takes decreasing values for decreasing ρ_3 and is smaller than the percolation value $\beta_{perc} = 5/36 \simeq 0.139$. Note that these results have to be treated with caution: (i) the data points cover less than a decade. (ii) Although the fitted power laws lie within the error bars, there appears to be a slight increase in slope with decreasing $(\rho_1 - \rho_1^c(\rho_3))/\rho_1$ for all three data sets. (iii) The data are taken relatively far away from the critical point $m = 0$, in fact probably already outside of the scaling regime. (Attempts to obtain scaling collapses of the data using the general scaling form given above did not work very well.) The exponent β, is actually only defined near $m = 0$ as as

$$[d \ln m / d \ln((\rho_1 - \rho_1^c(\rho_3))/\rho_1)]_{m=0} \,.$$

(iv) The simulated system is rather small. It is known from other nonequilibrium systems with quenched disorder [11] that finite size effects tend to be rather large and result in somewhat shifted values for the critical exponents. Curiously, in [11] collapses for the magnetization curves seemed also to be the hardest to obtain. (v) With increasing $(\rho_1 - \rho_1^c)$, the exponent β may cross over to some other value β'. In fact, our scaling theory (see Sect. 4.3) suggests that in the low disorder regime, very close to depinning, $((\rho_1 - \rho_1^c(\rho_3))/\rho_1 \ll (\rho_1^c)^{x/z}$, where x/z is a universal exponent estimated in Sect. 4.3), one has $m \sim ((\rho_1 - \rho_1^c(\rho_3))/\rho_1)^{\beta_{perc}}$ with $\beta_{perc} = 5/36$; and further away $((\rho_1^c)^{x/z} \ll (\rho_1 - \rho_1^c(\rho_3))/\rho_1$), one has $m \sim ((\rho_1 - \rho_1^c(\rho_3))/\rho_1)^{\beta'}$ with $\beta' = 0$. Such a scenario would explain the apparent decrease of β with decreasing disorder. Below, in Section 4, we will give analytical arguments that for small enough $\rho_1 - \rho_1^c$ the exponent β is identical to the percolation exponent. Furthermore, using a test simulation of another system for which β is known to be equal to β_{perc}, we will show that corrections to scaling tend to bias the numerically observed value for β towards a "wrong" value $\beta < \beta_{perc}$.

Nevertheless, a few valid conclusions can be derived from the numerical data. First, at least for $m > 0.5$ there seems to be no tendency to approach a finite saturation value of m. If this tendency continues for smaller values of m, it indicates a continuous depinning transition. Second, the critical interval $\rho_1 - \rho_1^c(\rho_3)$, for which m is smaller than some threshold value (*e.g.*, 0.5), becomes smaller with decreasing ρ_3. Our conclusion will be that for sufficiently small $\rho_1 - \rho_1^c$ the exponent β does not decrease with ρ_3, but that the *amplitude* of the power law has to increase with decreasing ρ_3. Below, the size of the critical region will be estimated using two different arguments, leading to a power-law divergence of the amplitude as $\rho_3 \to 0$. Third, using finite-size scaling, the fractal dimension of the invaded region can be estimated. The result is compatible with the percolation value $D_f = 91/48 \simeq 1.896$, as found earlier in [2,8].

3.3 The unflipped regions left behind

Figure 9 shows the size distribution $n(s)$ of unflipped domains behind the interface for $\rho_3 = 0.2$ and different values of ρ_1 close to ρ_1^c. The size is defined as the number s of unflipped spins within the domain. Unflipped spins that are nearest or next-nearest neighbours are defined to belong to the same domain. (This definition allows for system spanning clusters of unflipped spins coexisting with system spanning clusters of flipped spins at the depinning point). Near depinning we tested the scaling ansatz $n(s) \sim 1/s^\tau f_n(((\rho_1 - \rho_1^c)/\rho_1)^{\sigma_n} s)$ with f_n an appropriate

scaling function. This ansatz seems to give a collapse for $\tau = 1.85$, $\sigma_n = 1.8$, and $\rho_1^c = 0.437$ (see inset). This apparent scaling behaviour, however, cannot hold for very small $(\rho_1 - \rho_1^c)/\rho_1$, since the integral $\int_1^\infty sn(s)ds$ must be normalized to 1, allowing either for a scaling form with $\tau = 2$, or for $\tau < 2$ with no universal scaling behaviour. We can rule out the possibility $\tau > 2$, since the simulations as well as the analytical arguments below suggest that the total area of small unflipped regions decreases at the expense of large unflipped regions as ρ_1 approaches ρ_1^c. A value $\tau > 2$, in contrast, would imply that the area fraction covered by large unflipped regions is negligible.

Indeed, with decreasing distance from the critical value $\rho_1^c(\rho_3)$, the curve becomes flatter and does not converge to an asymptotic curve with finite cutoff. This behaviour can be interpreted as another indication that the order parameter vanishes when the critical point is approached. If it did not vanish, the size distribution of unflipped domains would approach some limit distribution with a finite cutoff at the critical point. Why this does not happen for a vanishing order parameter, is best illustrated for the site percolation limit of large disorder, $\rho_1 = p$, $\rho_4 = 1 - p$. There, the invaded area is identical (except for the first few columns) to the infinite percolation cluster. Clearly, as p is decreased towards its critical value $p_c \simeq 0.59$, larger and larger branches of the infinite percolation cluster become disconnected from it and are therefore no more flipped. All the unflipped domains formerly contained within this branch fuse, and larger unflipped domains are formed at the expense of smaller domains.

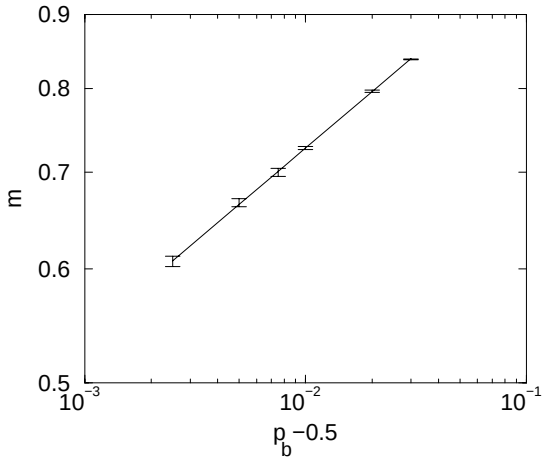

Fig. 10. Fraction of invaded sites for bond percolation with $L = 3200$, from a simulation with $\rho_1 = p_b$, $\rho_2 = p_b(1-p_b)$, $\rho_3 = p_b(1-p_b)^2$, $\rho_4 = (1-p_b)^3$, with $p_b = p_b^c = 1/2$. The solid line is a power law fit with the exponent $\beta = 0.1296$.

4 Analytical results

4.1 The exponent β

The simulation results shown in Figure 8 give a value of β, somewhere between 0.076 and 0.124, depending on ρ_3. The obtained range does not include the percolation value, which is $\beta_{perc} = 0.139$. As argued in Section 3.2, the data however are not conclusive, and a universal value $\beta = \beta_{perc}$ (or a close value) cannot be ruled out. A value β different from β_{perc}, would mean that any deviation of the densities ρ_n from the percolation values should be a relevant perturbation of percolation theory. In other words, the conditional flipping of spins depending on the number of flipped neighbours (*i.e.* $\rho_2 \neq 0$, $\rho_3 \neq 0$), should change the universality class. The case that β would depend on ρ_3 is highly unlikely. It would imply that even the extent to which spins are flipped as function of the state of their neighbours, would affect the value of the critical exponent.

In the following we give several points on the critical surface apart from $\rho_1 = 0.59...$, $\rho_4 = 1 - \rho_1$ where we can show by an analytic mapping onto percolation models that $\beta = \beta_{perc}$. These results will provide a strong case that β is indeed universal. One such point is given by $\rho_1 = p_b$, $\rho_2 = p_b(1-p_b)$, $\rho_3 = p_b(1-p_b)^2$, $\rho_4 = (1-p_b)^3$, with $p_b = p_b^c = 1/2$ being the critical threshold for bond percolation on a square lattice. In order to understand this, consider a bond percolation problem, where a pair of neighbouring sites is connected by a bond with probability p_b. We start with a row of up-spins at one end of the system and allow the avalanche to proceed to any site that can be accessed via open (*i.e.* existing) bonds. Some sites are invaded at the first nearest-neighbour contact with the spin-flip avalanche, others at the second contact, still others at the third contact, and the rest not even at the third contact. Obviously, the proceeding avalanche cannot distinguish whether it moves through a bond percolation system or a system with sites of different "colours" that are assigned according to the probabilities ρ_n (Eq. (4)). Clearly, the invaded bonds will form a bond percolation cluster. Since bond percolation can be mapped onto site percolation on a different lattice [17], and since the site percolation critical exponents do not depend on the lattice type, the number of invaded bonds diverges as $n_b \approx C(p_b - p_b^c)^{\beta_{perc}}$. In [20], it is proven that the number of invaded sites in a bond percolation problem increases with the same exponent as the number of invaded bonds. Consequently, the order parameter exponent is identical to β_{perc} for the above choice of the ρ_n.

Figure 10 shows the number of invaded sites as function of $p_b - p_b^c$. The simulations were performed by setting $\rho_1 = p_b$, $\rho_2 = p_b(1-p_b)$, $\rho_3 = p_b(1-p_b)^2$, $\rho_4 = (1-p_b)^3$, with $p_b = p_b^c = 1/2$ in the previous simulations. The solid line is a power-law fit to the data, with an exponent $\beta = 0.1296$, which is smaller than the true exponent $\beta_{perc} = 5/36 \simeq 0.139$ which we obtained from analytical arguments. This suggests that corrections to scaling modify the asymptotic power law to an apparently different power law further away from the critical point. Not shown in the figures is the result for the fractal dimension of the interface, which is again 4/3, as in the previous simulations. We therefore have strong reasons to believe that the bond percolation case discussed in this subsection belongs to the same universality class as the simulations described in the previous section.

For other special values of the densities ρ_n, mappings on various other types of percolation are possible. For example, site-bond percolation (*i.e.*, bond percolation where only the fraction p_s of all sites are accessible) interpolates between site percolation and bond percolation and is obtained for the densities $\rho_1 = p_s p_b$, $\rho_2 = p_s p_b(1-p_b)$, $\rho_3 = p_s p_b (1-p_b)^2$, and $\rho_4 = p_s(1-p_b)^3 + (1-p_s)$. Mappings on short-range correlated bond percolation are also possible, where the probability that a bond is open depends on the number of bonds pointing to the same site (in this situation, bonds must be given an orientation).

To summarize, there is strong evidence that the critical exponent β is indeed universal and identical to its percolation value 5/36.

4.2 The size of the critical region

As shown in Figure 8 and mentioned in Section 3.2, the parameter interval during which the order parameter increases from zero to a given finite value becomes smaller with decreasing disorder strength. Together with the results of the previous section, this suggests the form (for $(\rho_1 - \rho_1^c)/\rho_1 \ll (\rho_1^c)^{x/z}$)

$$m \simeq C \rho_3^{-\kappa} ((\rho_1 - \rho_1^c(\rho_3))/\rho_1)^{\beta}\,, \tag{7}$$

with $\beta = \beta_{perc} = 5/36 \simeq 0.139$, and with some exponent κ. In the following, we will first derive an estimate of the size of the critical region and of κ based on the understanding that the invaded area is a coarsened percolation cluster, and then a different estimate that is based on a study of the unflipped domains. Both estimates agree within 12 percent, suggesting that the true value is of the same order as the estimated values.

4.2.1 Arguments from percolation theory

From the previous section, we know that the invaded area can be viewed as an infinite percolation cluster with additional sites added to it. Since a spin-flip avalanche can only be stopped by "grey" sites that occur with a probability ρ_3^{-1}, we assume now that to each site of the infinite percolation cluster all sites within a distance ρ_3^{-1} are also flipped. This assumption is supported by the result in [8] that the "finger width" diverges roughly as ρ_3^{-1}. Clearly, when this distance becomes larger than the percolation correlation length ξ, practically all spins are flipped, and the system is no more in the critical region. We therefore find

$$((\rho_1 - \rho_1^c(\rho_3))/\rho_1)^{-\nu} \propto \rho_3^{-1}$$

at the boundary of the critical region, with $\nu = 4/3$ known from percolation theory, leading to a size of the critical region

$$((\rho_1 - \rho_1^c(\rho_3))/\rho_1) \propto \rho_3^{3/4}\,. \tag{8}$$

At the boundary of the critical region, m has some finite value, and setting m constant in equation (7), we find $\kappa/\beta = 3/4$, or

$$\kappa = 3\beta/4 = 5/48 \simeq 0.104\,. \tag{9}$$

4.2.2 Arguments using unflipped domains

Let us now consider the unflipped domains left behind by the infinite avalanche, and let us measure all distances in units of the "step size" $l \simeq 1/\rho_1$. The probability that a (pinning) path of a given step number k has its final point within unit distance l from the initial point is independent of the step size l for large l. Since there are of the order l^2 sites within distance l from the initial point, the probability that a path of k steps forms a closed loop vanishes as l^{-2}, which is proportional to ρ_3. On the other hand, there is a cutoff $1/(1 - p_{surv}/\rho_1)$ to the number of steps of a pinning path (see Eq. (5)), leading to

$$k_{max} \propto [(\rho_1 - \rho_1^c(\rho_3))/\rho_1]^{-1}$$

for small ρ_3. As long as there exists only small and rare unflipped domains, the system is beyond the critical region. The critical region can be characterized by the condition that the distance covered by a pinning path, $k_{max}^{3/4}$, becomes of the same order as the distance between unflipped domains. Then, the picture of rare independent unflipped domains is no longer valid, since these domains can be connected by pinning paths, leading to a divergence of the size of unflipped domains. The above condition reads

$$k_{max}^{3/4} \propto l \propto \rho_3^{-1/2}\,,$$

and gives the following estimate of κ by again putting $m = const$ and using the assumption of equation (7)

$$\kappa = 2\beta/3 = 5/54 \simeq 0.093\,. \tag{10}$$

This argument also shows that the size distribution of unflipped domains does not converge towards a fixed function with finite cutoff for $\rho_1 \to \rho_1^c(\rho_3)$, but rather that small unflipped domains become connected to form large unflipped domains, as observed in the simulations.

4.3 Scaling theory

The results for the order parameter and the unflipped domains lead to a scaling theory that is similar in spirit to the one proposed in [21] for the equilibrium random-field Ising model in two dimensions at low disorder. We introduce the scaling variable

$$h = (\rho_1 - \rho_1^c)/\rho_1,$$

which measures the distance from the depinning threshold and is roughly equivalent to $(H/R - H_c/R)$, and

$$t = \rho_1^c\,,$$

which is a measure for the disorder strength and is to leading order

$$\rho_1^c \simeq \sqrt{\rho_3} \propto \exp[-0.343 J^2/R^2]\,.$$

The characteristic length scale t^{-1} is the length of straight interface segments. The correlation length ξ is most naturally identified with the diameter of the largest unflipped domain, weighted by the density of these domains, and can be expected to scale with some power of t. In equilibrium, the correlation length scales also as $\exp[CJ^2/R^2]$, with a constant C different from the depinning problem.

Under coarse graining, the scaling variables change to

$$h' = b^x h, \qquad t' = b^z t.$$

We assume that the exponent x is $x = d - d/2 = 1$, because the renormalized external field H and random fields $\{h_i\}$ are given by the sum of the corresponding fields in the cell, leading to dimensions d and $d/2$ respectively [21]. Here, the main assumption is that we can apply equilibrium rescaling under coarse graining to this essentially non-equilibrium problem. The reasoning is that in the limit of low disorder almost all (except for a vanishing fraction as $R \to 0$) coarse grained "block spins" flip *coherently* thereby optimally lowering their local energy, and obeying essentially the same rules as single spin flips on shorter length scales. The exponent z will be related below to the exponent κ. The correlation length ξ and the order parameter m transform under coarse graining according to

$$\xi' = \xi(t', h') = b^{-1}\xi(t, h)$$

and

$$m' = m(t', h') = b^y m(t, h)$$

with $y = 0$ (since all spins within a box of size b^2 are parallel at $t = 0$), leading to

$$\xi \simeq t^{-1/z}\tilde{\xi}(h/t^{x/z})$$

and

$$m \simeq t^{y/z}\tilde{m}(h/t^{x/z}).$$

As is seen from Figure 11, on long length scales the system flows to the percolation fixed point at infinite disorder. The zero disorder fixed point and the percolation fixed point are connected by the depinning critical line which is described by the correlation critical fixed points on sufficiently long length scales. In the following we use information about the percolation fixed point to extract the asymptotic behaviour of the scaling functions as well. For $h \ll t^{x/z}$, we expect

$$\tilde{\xi} \sim (h/t^{x/z})^{-\nu}$$

with $\nu = \nu_{perc} = 4/3$, or

$$\xi \propto h^{-\nu} t^{(x\nu - 1)/z}\,.$$

For smaller disorder, ξ is also smaller (for the same value of h), in agreement with our previous finding that the width of the critical region becomes smaller.

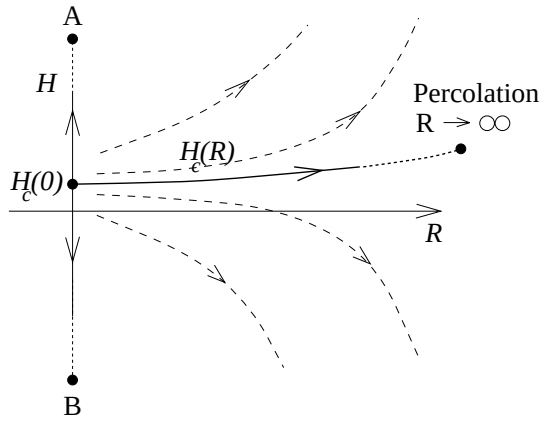

Fig. 11. Sketch of the flowdiagram for the order parameter. There are 4 fixed points in this diagram: at $R = 0$, $H = H_c(0)$ (with $H_c(0) = 1.172J$ for the model discussed here), which is the zero disorder fixed point discussed in this paper; at finite H, $R \to \infty$, which is the percolation fixed point; and at $H = \pm\infty$, $R = 0$ (A and B), which attract all the flow above respectively below the critical line. These two fixed points correspond to a completely flipped system and to a system that is not invaded at all. The thick line marked $H_c(R)$ is the depinning line. The arrows indicate the direction of flow under coarse graining. The diagram explains why systems very close to $H_c(R)$ are dominated by percolation critical exponents on long length scales, as discussed in the paper.

From the previous section we know that for $h \ll t^{x/z}$

$$\tilde{m}(h/t^{x/z}) \sim (h/t^{x/z})^{\beta}$$

with $\beta = \beta_{perc}$. This gives for $h \ll t^{x/z}$

$$m \sim t^{(y-\beta x)/z} h^{\beta}$$

and the scaling relation

$$\kappa = (\beta x - y)/2z.$$

Inserting the known values for the exponents y, x, and β, the relation between κ and z becomes

$$z = 5/72\kappa\,.$$

The two above estimates for κ give then $z = 4/7$ or $z = 9/14$.

In the opposite limit $h \gg t^{x/z}$, the order parameter saturates at 1, *i.e.*,

$$\tilde{m}(h/t^{x/z}) \sim (h/t^{x/z})^{\beta'}$$

with $\beta' = 0$. For intermediate values of $h/t^{x/z}$, the scaling function $\tilde{m}$ interpolates between the two limits. The exponent β' is also observed for faceted growth, where never more than two "colours" are present, and where depinning occurs at $\rho_2 = 1$. In the flow diagram, faceted depinning occurs at the left-hand fixed point, and the flow follows the perpendicular axis.

The correlation length ξ is close to zero for $h \gg t^{x/z}$, since essentially no unflipped domains are left behind. This means that the scaling function $\tilde{\xi}$ becomes proportional to $(h/t^{x/z})^{-\nu'}$, with $\nu' = \infty$.

5 Conclusions

The results of this paper confirm that 2 is the lower critical dimension for the transition from percolation-like to conventional depinning of a domain wall in the random-field Ising model. This conclusion is based on the numerical observation that the order parameter (the fraction of flipped spins) vanishes continuously as the depinning threshold is approached, even in the limit of very small disorder. Numerical results as well as analytical arguments show that the size distribution of unflipped domains left behind by the spin-flip avalanche becomes flatter closer to the depinning threshold, not allowing for a nonvanishing order parameter at the threshold.

Furthermore, this paper supports the hypothesis that the order parameter exponent β is the same as in uncorrelated site percolation. Since numerical data are not conclusive and rather indicate an exponent β that depends on the disorder strength, an explicit mapping of the infinite avalanche of the depinning problem onto an infinite cluster in percolation theory is performed for several distinct parameter values. The reason why the asymptotic value of the critical exponent β cannot be seen in the simulations is that the width of the critical region shrinks to zero as the disorder strength vanishes. Analytical arguments in this paper estimate the value of the exponent that characterizes the width of the critical region, and lead to a scaling theory that relates this exponent to other exponents.

As argued in [5], depinning in the random-field and random-bond Ising models belong to the same universality class, and the non-equilibrium random bond and random field Ising model have the same symmetries near the critical point (for the same reasons as given in [22]), we therefore expect that the results of this paper are also valid for the random-bond Ising model. In contrast, the equilibrium critical behaviour of the two models is different.

The question of the universality of the exponent β occurs also in the context of bootstrap and diffusion percolation [23], where all unoccupied sites of a site percolation problem that have a certain number of occupied neighbours are also occupied. Recently, evidence was found that the exponent β is universal in two dimensions [24].

The scaling theory presented in this paper discusses only the order parameter and correlation length in the bulk, after the spin-flip avalanche has transversed the system. The scaling behaviour of the front is somewhat simpler for small disorder, since for small t and h the correlation length is identical to the length of a pinning path, which is proportional to

$$(lk_{max})^{3/4} = (th)^{-3/4},$$

leading to a scaling variable th. A pinning path is essentially a self-avoiding random walk. Therefore the fractal dimension of the front is 4/3, which is different from the percolation value 7/4. However, close to the site percolation fixed point (*i.e.* for large disorder), a crossover between the two exponents should be observed. Curiously, this implies that the flow diagram for the correlation length of the front shows a flow from the percolation fixed point to the $t = h = 0$ fixed point, which is the opposite direction to the flow in Figure 11. A scaling theory for the front should therefore be performed in the neighbourhood of the percolation fixed point, which was not the focus of this paper. Other front properties like the size distribution of avalanches below the depinning threshold and the velocity of the front were not studied in this paper either and have still to be determined.

It is certainly possible to generalize the scaling theory of this paper for the transition from percolation-like to conventional depinning to the neighbourhood of two dimensions by performing a $2+\epsilon$ expansion, in a way similar as in [21] for the equilibrium model. An expansion around the upper critical dimension is a bigger challenge. Since in dimensions larger than 2 the disorder strength is not vanishingly small at the phase transition between the two different modes of depinning, the neglection of spontaneous spin flips away from the domain wall is realistic only under certain circumstances, for example for fluid invasion, for magnetic samples in a gradient field, or in the presence of certain long range interactions [22]. If, on the other hand, one includes these spontaneous spin flips, one arrives at a hysteresis model for which an expansion around the upper critical dimension 6 was successfully performed in [22].

We would like to thank A. Bray, J. Essam, T. Prellberg, and in particular J.P. Sethna for helpful discussions. This work was supported by EPSRC Grant No. GR/K79307, the Society of Fellows of Harvard University, and NSF *via* DMR 97-14725, 9630064, and Harvard's MRSEC.

References

1. T. Nattermann, Theory of the Random Field Ising Model, to appear in *Spin Glasses and Random Fields*, edited by P. Young (World Scientific, Singapore, 1997).
2. H. Ji, M.O. Robbins, Phys. Rev. A **44**, 2538 (1991).
3. N. Martys, M.O. Robbins, M. Cieplak, Phys. Rev. B **44**, 12294 (1991).
4. T. Nattermann, S. Stepanow, L.H. Tang, H. Leschhorn, J. Phys. II France **2**, 1483 (1992).
5. O. Narayan, D.S. Fisher, Phys. Rev. B **48**, 7030 (1993).
6. H. Leschhorn, T. Nattermann, S. Stepanow, L.-H. Tang, Ann. Physik, **6**, 1 (1997).
7. H. Ji, M.O. Robbins, Phys. Rev. B **46**, 14 519 (1992).
8. B. Koiller, H. Ji, M.O. Robbins, Phys. Rev. B **46**, 5258 (1992).
9. B. Koiller, H. Ji, M.O. Robbins, Phys. Rev. B **45**, 7762 (1992).
10. G. Aeppli, R. Bruinsma, J. Magn. Magn. Mat. **54**, 25 (1986).
11. O. Perković, K.A. Dahmen, J.P. Sethna, Phys. Rev. Lett. **75**, 4528 (1995), and preprint cond-mat/9609072 (1996).
12. O. Narayan, D.S. Fisher, Phys. Rev. Lett. **68**, 3615 (1992); Phys. Rev. B **46**, 11520 (1992); Phys. Rev. B **48**, 7030 (1993) (CDW); C. Myers, J.P. Sethna, Phys. Rev. B **47**, 11171 (1993), and Phys. Rev. B **47**, 11194 (1993) (CDW); O. Narayan, A.A. Middleton, Phys. Rev. B **49**, 244 (1994) (CDW); D. Cule, T. Hwa, Phys. Rev. Lett. **77**, 278 (1996)

(earthquakes); D.S. Fisher, K. Dahmen, S. Ramanathan, Y. Ben-Zion, Phys. Rev. Lett. **78**, 4885 (1997) (earthquakes); D. Ertaş, M. Kardar, Phys. Rev. E **49**, R2532 (1994) (contact lines).
13. S. Zapperi, Pierre Cizeau, G. Durin, H. E. Stanley, Phys. Rev. Lett. **79**, 4669 (1997).
14. M.O. Robbins, private communication.
15. L.-H. Tang, M. Kardar, D. Dhar, Phys. Rev. Lett. **74**, 920 (1995).
16. $R_c = 0$ needs not necessarily be true for a lower critical dimension. The Kosterlitz Thouless transition [25], for example occurs at the lower critical dimension at a nonzero critical temperature.
17. D. Stauffer, A. Aharony, *Introduction to percolation theory*, revised second edition (Taylor & Francis, London, Bristol, PA 1994).
18. The probabilities ρ_1 and ρ_3 correspond to f_l and $(1 - f_u)$ in [8], and to p_1 and p_0 in [19].
19. R. Blossey, T. Kinoshita, J. Dupont-Roc, Physica A **248**, 247 (1998).
20. J. Blease, J.W. Essam, C.M. Place, Phys. Lett. A **57**, 199 (1976).
21. A.J. Bray, M.A. Moore, J. Phys. C **18**, L927 (1985).
22. K. Dahmen, J.P. Sethna, Phys. Rev. B **53**, 14 872 (1996); Phys. Rev. Lett. **71**, 3222 (1993); K. Dahmen, Ph.D. thesis, Cornell University, 1995.
23. J. Adler, Physica A **171**, 453 (1991).
24. C.M. Chaves, B. Koiller, Physica A **218**, 271 (1995).
25. J.M. Kosterlitz, D.J. Thouless, J. Phys. C, **6**, 1181 (1973).